WHEN AVALANCHES GET WETTER: ARE OUR BUILDING CODES FIT FOR THE FUTURE?

Michael L. Kyburz*[1,2,3], Stefan Margreth[1], Betty Sovilla[1], Johan Gaume[1,2,3]

[1]*WSL Institute for Snow and Avalanche Research SLF, Davos, Switzerland*
[2]*Climate Change, Extremes and Natural Hazards in Alpine Regions Research Center CERC, Davos, Switzerland*
[3]*Chair of Alpine Mass Movements, ETH Zürich, Zürich, Switzerland*

ABSTRACT: Avalanche impact pressures on structures remain challenging to predict because avalanche–structure interactions depend strongly on flow regime, snow properties and the geometry of the object. Current guidelines on structural actions predominantly estimate impact pressure using a hydrodynamic approach proportional to density and velocity squared. This approach may not adequately represent slow, wet avalanches, for which frictional, and cohesive effects can contribute substantially to the impact pressure. With wet-snow avalanches becoming more frequent in a warming climate, we assess the robustness and applicability of current guidelines on structural actions under such conditions. To achieve this, we use three-dimensional Material Point Method (MPM) simulations to investigate wet-snow avalanche impacts on structures representative of typical residential buildings. We compare the simulated pressures with predictions from current guidelines on structural actions and a recently proposed equation incorporating frictional and cohesive effects. Our results provide insight into the influence of avalanche width, flow velocity, and material cohesion on impact pressures. We find that the current guidelines generally underestimates impact pressures for slow avalanches, whereas including frictional and cohesive pressure contributions provides better agreement, particularly for wide avalanches. The simulations further reveal a strong dependence of impact pressure on the relative avalanche and structure widths, highlighting the importance of lateral confinement and the resulting mobilized domain in avalanche–structure interactions.

KEYWORDS: Wet avalanche impact loads; Guidelines on structural actions; 3D Numerical modelling; Material Point Method; Climate change

1. INTRODUCTION

Calculating avalanche impact pressures on structures is one of the most important engineering tasks in avalanche science. However, predicting these pressures remains challenging because avalanche–structure interactions involve a range of processes that are only partly understood. The complexity is further increased by the strong dependence of snow properties and avalanche flow regimes on ambient conditions, which can lead to substantial variations in avalanche dynamics and impact behavior.

Current guidelines on structural actions, including the Swiss SIA standards and European guidelines, generally estimate avalanche impact pressure using a hydrodynamic formulation (e.g. Gauer et al., 2009; SIA261/1, 2020). According to the Swiss guidelines on structural actions (SIA261/1, 2020), the pressure of a perpendicular impact of a dense avalanche flow on a “large building” wider than 5 m can be calculated as:

$$p_{hyd} = \frac{1}{2}\rho_a v^2 C_D, \quad (1)$$

where ρ_a is the avalanche density, v is the flow velocity, and C_D is a drag coefficient. For perpendicular impact of a dense avalanche on a “large building” wider than 5 m, the Swiss guidelines prescribe a drag coefficient of $C_D = 2$ (SIA261/1, 2020).

This formulation represents impact pressure purely as an inertial contribution and therefore implies that pressure decreases rapidly with decreasing avalanche velocity.

Field observations, however, have shown that slow, wet avalanches can exhibit a hydrostatic pressure profile that is not proportional to velocity (e.g. Sovilla, Kern, et al., 2010), but to flow height. Such effects are often neglected in current guidelines. In recent years, research has therefore focused on identifying the processes governing avalanche–structure interactions and quantifying their contributions to the resulting impact pressure. Based on conceptual and experimental studies (Faug, 2015; Thibert and Baroudi, 2010; Sovilla, Kern, et al., 2010), Kyburz, Sovilla, Gaume, et al. (2020) interpreted avalanche impact pressure as the sum of three contributions. The relative

* *Corresponding author address:*
Michael L. Kyburz, WSL Institute for Snow and Avalanche Research SLF,
Flüelastrasse 11, 7260 Davos Dorf;
email: michael.kyburz@slf.ch

https://doi.org/10.15788/1790098848

importance of the contributions depends on the flow regime, characterized by the Froude number $Fr = v/\sqrt{gh}$, which provides a measure of the balance between inertial and gravitational effects. The concept of the mobilized domain (Faug, 2015; Kyburz, Sovilla, Gaume, et al., 2022b) further provides a framework to account for the mass of snow mobilized during the interaction. Building on these developments, Kyburz, Sovilla, Gaume, et al. (2022a) proposed a pressure calculation approach that extends the purely hydrodynamic approach by explicitly incorporating granular and cohesive effects:

$$p_{kyb} = (\frac{\rho_a}{2} v^2 \, C_D) \cdot f_c \tag{2}$$

where f_c is the cohesion amplification factor, typically in the range between 1 and 2.5, and the drag coefficient is defined as $C_D = C_w C_o (1 + C_o/Fr^2)$ with coefficients C_w depending on the width of the structure and C_o depending on the geometry of the structure. Consistent with (SIA261/1, 2020), $C_o = 2$ for perpendicular impact on a flat wall. As the study Kyburz, Sovilla, Gaume, et al. (2022a) focused on impact on narrow obstacles $C_w \approx 1$ was considered for structures wider than 6 m.

Direct field measurements of avalanche impacts on structures representative of residential buildings remain difficult and costly because of the large forces involved. Numerical simulations therefore provide a valuable complementary approach for investigating the underlying interaction processes. In this study, we use the Material Point Method (MPM) (Gaume et al., 2018) to simulate snow avalanche impact on structures with dimensions of typical residential buildings targeted by current building codes. In particular, in this study we consider the characteristic parameters of the material and avalanche flow of wet-snow avalanches and compare the resulting impact pressures with those predicted by current guidelines on structural actions and the approach of Kyburz, Sovilla, Gaume, et al. (2022a), which accounts for granular and cohesive effects.

2. SETUP AND METHOD

2.1. Numerical Method

In this study, we use the fully three-dimensional SLAB3D code based on the Material Point Method (MPM) (Gaume et al., 2018). MPM is a hybrid method, where the mass, displacement and velocity are tracked with Lagrangian material points and stresses and deformations are calculated on an Eulerian background grid. To simulate a particular material in MPM, constitutive models are implemented in an elastoplastic framework. In this study, the constitutive model is the Modified Cam Clay (MCC) model (Gaume et al., 2018), which yielded good results in reproducing the granular flow characteristics of snow avalanches (e.g. Li et al., 2020; Kyburz, Sovilla, Bühler, et al., 2025), as well as capturing snow compressibility and avalanche–structure interactions (e.g. Ceccato et al., 2018; Kyburz, Margreth, et al., 2024; Kohler et al., 2026b). To model wet snow with MCC, we use a range of values typical of wet snow and other avalanche simulations (e.g. Li et al., 2020; Kyburz, Sovilla, Bühler, et al., 2025; Kohler et al., 2026b). We summarize the most important material parameters in Table 1.

Table 1: MCC constitutive parameters for wet snow.

Quantity	***Symbol***	***Unit***	***Values***
Youngs's modulus	E	MPa	1
Density	ρ	kg/m^3	300
SCL*	M	-	0.8
Pre-consolidation	p_0	kPa	15
Cohesion†	c	kPa	0.0, 3.75
Hardening coeff.	ξ	-	0.2

*Slope of Critical state Line

† $c = \beta \, p_0$, where we choose $\beta = 0.0, \, 0.25$

2.2. Simulation Setup

For the present study, we use a simple setup visualized in Figure 1 of a building represented by a cube of width W 10 m and 20 m. The height H is high enough to prevent overflowing. We only consider perpendicular impact on a flat plane. Due to lack of slope, we prescribe the velocity of the snow release at an upstream distance greater than 2.5 times the structure width W. The material closer to the structure flows and interacts freely with the structure.

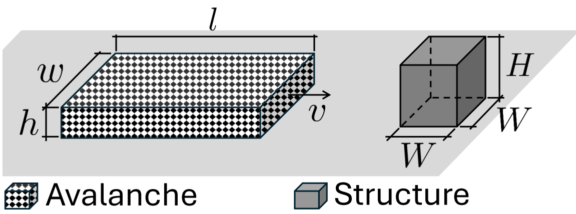

Figure 1: Schematic sketch of the numerical setup with the glide plane in light gray, the structure in dark gray and the snow avalanche volume checkered. The objects are not to scale.

In our study, we use typical wet snow avalanche characteristics, such as flow heights h of 1, 3 and

5 m, avalanche widths w of 10 m, 50 m and 100 m, a volume of 50'000 m^3, as well as velocities v between 3 and 10 m/s. However, not all combinations of these parameters are simulated, as for certain combinations the avalanche volume becomes very elongated, short or the interaction time with the structure is too short to obtain a representative impact pressure value.

In the simulations the impact force is evaluated as the integral reaction force on the whole structure. The simulated impact force varies over time as shown for two exemplary simulations in Figure 2. To be able to compare the impact force and pressure between different simulations, we extract a single value per simulation by taking the 90-percentile value of the whole time series. To obtain a pressure value, we divide the impact force by the structure width W and the *pressure height* (Kohler et al., 2026a), which is the vertical extent over which significant impact pressure, $> 5\%$ of the depth-averaged pressure within distance h from the ground, acts on the structure. In our analysis, we discard simulations, where the automatically detected pressure height is $\leq 80\%$ than the avalanche flow height h, because this is considered unrealistic and leads to excessively high impact pressures. All simulations are stopped after a simulated time of 30 s.

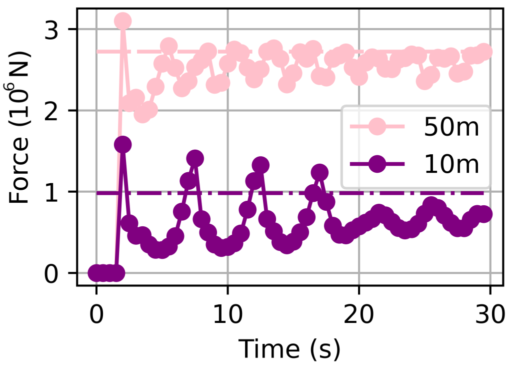

Figure 2: Time series (dots and continuous line) of simulated of impact force on 10 m-wide structure for 10 m and 50 m wide avalanche and representative force value (dash-dotted line) based on the 90-percentile criterion.

3. RESULTS

We first investigate how avalanche width affects the interaction with a 10 m-wide structure. Figures 3 a-b show two representative simulations of cohesive avalanches with $c = 3.75$ kPa, $h = 5$ m, and $v = 5$ m/s, with avalanche widths of $w = 10$ m and $w = 50$ m, respectively. For the 10 m-wide avalanche (Figure 3 a), the avalanche initially impacts the structure perpendicularly but is subsequently deflected laterally by the deposits that accumulate upstream of the structure. The inset illustrates that a similar deflection can occur for narrow wet-snow avalanches even in the absence of a structure. Figure 2 shows that the impact force may exhibit considerable oscillations. The fluctuations characterizing the purple curve demonstrate that the deflected flow is not stationary. As material accumulates on the side toward which the avalanche is deflected, the flow may become temporarily blocked, causing it to recenter on the structure or switch entirely to the opposite side. Even during deflection, the impact pressure does not decrease to zero, because residual stresses are transmitted to the structure through the static deposits.

In contrast, the 50 m-wide avalanche forms a pronounced stagnation zone, or mobilized domain (Thibert, Faug, et al., 2013; Faug, 2015; Sovilla, Faug, et al., 2016; Kyburz, Sovilla, Gaume, et al., 2022b), upstream of the structure. The wider avalanche laterally confines this domain as the flow continues around both sides of the structure. Time variations in the force signal in this configuration (pink curve in Figure 2) most probably originate from the well-known frictional and jamming processes in the mobilized domain (Albert et al., 2000; Sovilla, Kern, et al., 2010; Kyburz, Sovilla, Gaume, et al., 2022b).

Figures 3 c-d compare the simulated impact pressure p_{sim} with pressures calculated using equations (1) and (2) for varying avalanche velocities. We consider both non-cohesive avalanches ($c = 0.0$ kPa, empty circles) and cohesive avalanches ($c = 3.75$ kPa, filled squares). The simulated pressure remains approximately constant even as the velocity increases to 10 m/s, whereas both equations (1) and (2) predict a stronger velocity dependence. The relatively large difference between p_{sim} and calculated pressures for $v > 5$ m/s deserves further investigation.

For the 10 m-wide avalanches (Figure 3 c), cohesive avalanches produce almost twice the impact pressure of non-cohesive avalanches for velocities $v \leq 5$ m/s. This difference decreases at higher velocities. Equation (2) reproduces the same qualitative trend, but consistently predicts higher pressures than the simulations for both, non-cohesive and cohesive avalanches. In contrast, equation (1) underestimates p_{sim} for all velocities and cohesion values except for the non-cohesive avalanche at $v = 10$ m/s.

For the 50 m-wide avalanches (Figure 3 d), the

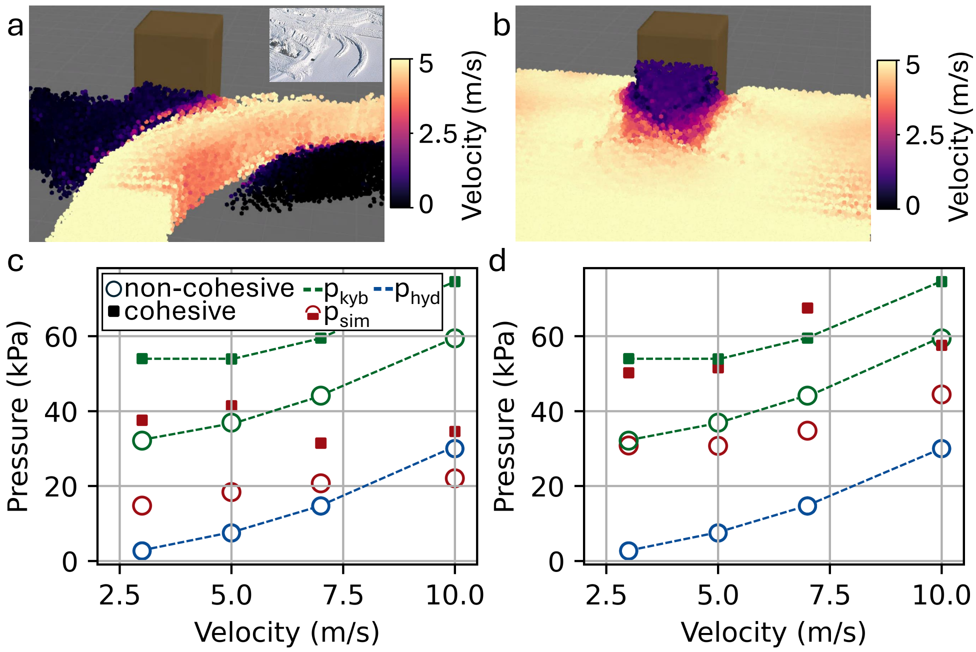

Figure 3: (a) Simulated impact of 10 m-wide and (b) 50 m-wide avalanche on a 10 m-wide structure (brown). The inset in panel a shows the run-out of wet-snow avalanche fingers on an open field (Picture: SLF, S. Margreth). (c) Comparison of simulated and calculated impact pressures for varying velocity of 10 m-wide and (d) 50 m-wide avalanche on a 10 m-wide structure.

calculated pressures from equations (1) and (2) remain identical to those in panel c because neither equation explicitly accounts for avalanche width. However, the simulated impact pressure increases considerably with avalanche width. For these wider avalanches, values obtained from equation (2) agree well with p_{sim} and capture the difference between cohesive and non-cohesive material. Equation (1), in contrast, considerably underestimates p_{sim} for all cases, although the discrepancy decreases with increasing velocity.
We quantify this discrepancy by calculating relative error between the simulated pressure and the values calculated from equations (1) and (2) for 10 m-wide structures and non-cohesive and cohesive avalanches with $v = 3 - 10$ m/s and $h = 1 - 5$ m. The results in Figure 4 a and b show that, despite some outliers, the relative error between simulated and calculated pressure is generally below 1.7. Analyzing the relative error confirms the same general tendency as visible in Figure 3 c and d, where for $v \leq 5$ m/s, p_{kyb} generally provides a closer estimate of p_{sim} than p_{hyd} for both, non-cohesive and cohesive avalanches. At higher velocities, this trend reverses. The large relative error between p_{sim} and p_{kyb} for $v > 5$ m/s may be related to the relatively low simulated impact pressure simulated in MPM, as mentioned above. Figure 5 a shows the simulated impact pressure for different structure-to-avalanche-width-ratios W/w colored by the flow height, across the range of flow conditions described in Section 2.2. We observe a clear decrease in p_{sim} with increasing W/w. This confirms the trend observed in Figure 3 c and d: for a structure of constant width, a narrower avalanche produces lower impact pressure. The results in Figure 5 indicate that, more generally, the relative widths of the structure and avalanche, rather than their absolute widths alone, strongly influence the impact pressure. The absolute pressure p_{sim} changes for varying flow height but the trend persists for cohesive and non-cohesive flows as well as different flow heights.
The remaining scatter of the data originates from the differing flow velocities. We show this for the exemplary case of $h = 1$ m, $W = 20$ m by coloring the data points by velocity in Figure 5 b. As expected for slow avalanches ($Fr < 1$) the influence of velocity on the impact pressure is weaker than the influence of the flow height. Nevertheless, Figure 5 b clearly shows that the tendency of decreasing p_{sim} persists also for a flow height as low as $h = 1$ m.

4. DISCUSSION AND CONCLUSIONS

The simulated impact pressures fall within a physically reasonable range, but experimental data, ideally from full-scale experiments, are

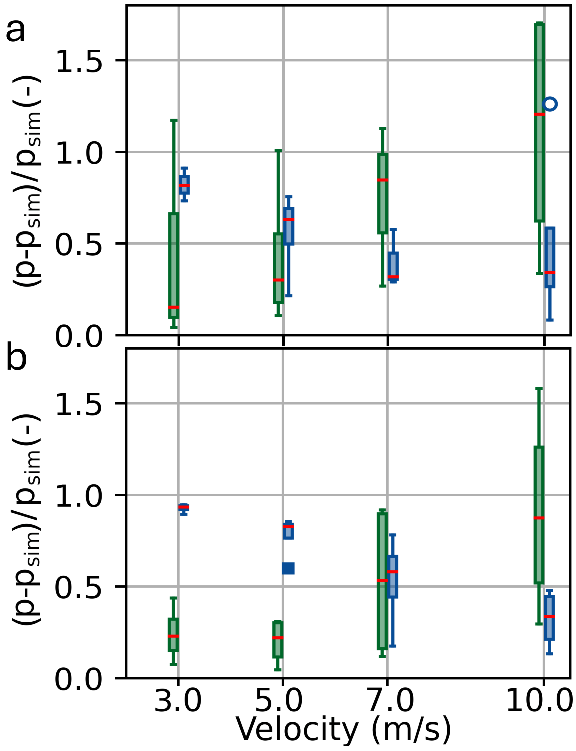

Figure 4: Panels a and b show boxplots of relative error between p_{kyb} and p_{sim} (green), as well as p_{hyd} and p_{sim} (blue) for impacts of cohesive and non-cohesive avalanches, respectively. The median value is marked with the red lines and outliers with single markers of the corresponding color.

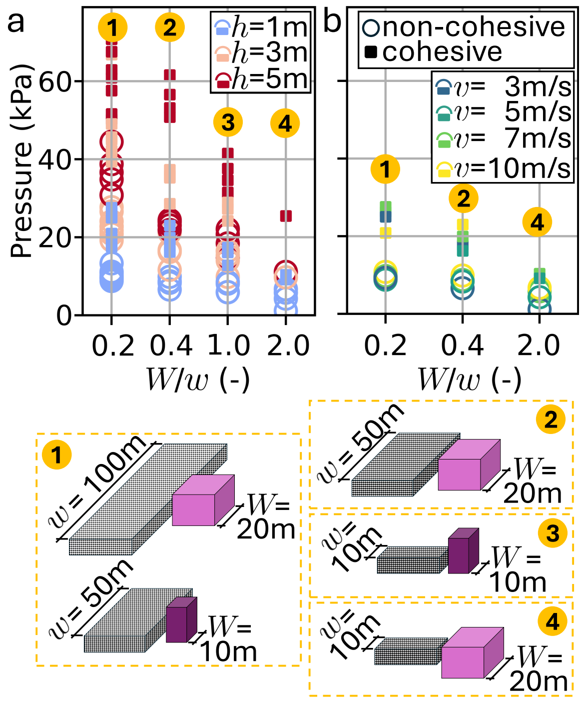

Figure 5: Panel a shows simulated impact pressure against W/w for various v, colored by flow height h. Panel b shows simulated impact pressure against W/w for the case of $h = 1$ m, $W = 20$ m with the data points colored by velocity. In both panels, empty circles mark non-cohesive avalanches ($c = 0.0$ kPa) and filled squares mark cohesive avalanches ($c = 3.75$ kPa). Panels 1-4 at the bottom illustrate the different W/w combinations indicated in the plots above.

required to validate the individual pressure values. We therefore do not interpret the simulations as providing highly accurate absolute pressure predictions. Instead, we focus on the robust tendencies that persist across the range of material parameters.

The simulations consistently show that equation (1) from the current guidelines on structural actions underestimates impact pressure for slow avalanches ($v < 5$ m/s). This discrepancy results from the omission of cohesive and frictional effects in equation (1). Accounting for these additional contributions, as in the approach of Kyburz, Sovilla, Gaume, et al. (2022a), reduces the discrepancy with the simulated pressures. In particular, for wide avalanches, or when the structure is narrow relative to the avalanche width, the proposed calculation method, originally developed for narrow obstacles, provides good agreement with the simulations, whereas the current guidelines considerably underestimates the pressure.

The dependence of p_{sim} on W/w is likely the result of the influence of the lateral confinement of the avalanche near the structure. We can identify two limiting configurations: a laterally unconfined case, in which the avalanche can spread freely, and a strongly confined case, in which the lateral extent of the avalanche itself constrains the material around the structure. While further in-depth investigation is needed, we assume that in the unconfined configuration, as soon as the stress in the material accumulating upstream of the structure reaches the yield stress, a local shear failure is induced and the incoming material is deflected to the side with little resistance. A wider avalanche, however, inhibits the lateral deformation due to the confinement and allows greater compressive stress to develop upstream of the structure, where the resistance to flow is low in the absence of lateral confinement.

In the Swiss guidelines on structural actions (SIA261/1, 2020), the structures are assumed to be infinitely wide. From practical experience, this assumption is mostly valid for $W > 5$ m, as stated in the guidelines, and $h \leq 2$ m is implicitly assumed for typical flow heights. However, this range of h is characteristic of dry dense avalanches and are likely larger in wet avalanches (e.g. Sovilla, Kern, et al., 2010). Moreover, Figure 5 b indicates, that the dependency of p_{sim} with W/w still holds for flow heights in the range of $h \leq 2$ m. In the light of these results and of wet avalanches becoming more frequent, the limit between "narrow", for which other guidelines exist (Margreth, 2007), and "wide" structures should be defined more precisely, possibly as a function of avalanche flow height and width.

The simulated setup and interaction mechanisms represent idealized cases. Conditions in the field are often more complex. For example, old avalanche deposits or a snow cover that remains in front of the structure could deflect even a wide avalanche and thereby reduce the impact pressure. In addition, we only consider perpendicular impacts, which represent a special case. As a continuation of this work, we will investigate impacts at an angle of 20°, corresponding to the impact-angle variation considered in the SIA guidelines on structural actions (SIA261/1, 2020).

In summary, our results suggest that hazard assessments for wet-snow avalanches should consider not only the inertial impact pressure p_{hyd} prescribed by current guidelines, but also potentially significant frictional and cohesive contributions. Avalanche width and, consequently, lateral confinement represent an additional important factor. Given the difficulty of predicting the effective avalanche width, hazard assessments may need to consider the conservative case of a highly confined avalanche–structure interaction. Although recent advances have improved our understanding of these processes, the complexity of avalanche–structure interactions and the remaining uncertainties warrant further investigation.

REFERENCES

Albert, I., Tegzes, P., Kahng, B., Albert, R., Sample, J. G., Pfeifer, M., Barabási, A.-L., Vicsek, T., and Schiffer, P. (May 2000). Jamming and Fluctuations in Granular Drag. In: Physical Review Letters 84 (22), pp. 5122–5125. https://doi.org/https://doi.org/10.1103/PhysRevLett.84.5122.

Ceccato, F., Redaelli, I., Prisco, C. di, and Simonini, P. (2018). Impact forces of granular flows on rigid structures: Comparison between discontinuous (DEM) and continuous (MPM) numerical approaches. In: Computers and Geotechnics 103, pp. 201–217. ISSN: 0266-352X. https://doi.org/https://doi.org/10.1016/j.compgeo.2018.07.014.

Faug, T. (2015). Macroscopic force experienced by extended objects in granular flows over a very broad Froude-number range. In: The European Physical Journal E 38.5, p. 34. ISSN: 1292-895X. https://doi.org/https://doi.org/10.1140/epje/i2015-15034-3.

Gauer, P. and Jóhannesson, T. (2009). "The design of avalanche protection dams Recent practical and theoretical developments". In: Climate Change and Environmental Risks. EUROPEAN COMMISSION. Chap. Loads on walls, pp. 77–94.

Gaume, J., Gast, T., Teran, J., Van Herwijnen, A., and Jiang, C. (2018). Dynamic anticrack propagation in snow. In: Nature communications 9.1, pp. 1–10. https://doi.org/https://doi.org/10.1038/s41467-018-05181-w.

Kohler, M. J., Gaume, J., Ancey, C., and Sovilla, B. (2026a). Distinguishing run-up height from pressure distribution during avalanche impact on narrow obstacles: mechanisms and semi-empirical prediction. In: EGUsphere 2026, pp. 1–28. https://doi.org/https://doi.org/10.5194/egusphere-2026-1181.

Kohler, M. J., Gaume, J., Ancey, C., and Sovilla, B. (2026b). 3D Numerical modeling of compressible and cohesive granular flow impact on narrow obstacles. In: Computational Particle Mechanics 13, pp. 79–96. ISSN: 2196-4386. https://doi.org/https://doi.org/10.1016/j.cpms.2025.11.005.

Kyburz, M. L., Sovilla, B., Gaume, J., and Ancey, C. (2020). Decoupling the role of inertia, friction, and cohesion in dense granular avalanche pressure build-up on obstacles. In: Journal of Geophysical Research: Earth Surface 125.2. e2019JF005192 10.1029/2019JF005192, e2019JF005192. https://doi.org/https://doi.org/10.1029/2019JF005192.

Kyburz, M. L., Sovilla, B., Gaume, J., and Ancey, C. (2022a). Physics-based estimates of drag coefficients for the impact pressure calculation of dense snow avalanches. In: Engineering Structures 254, p. 113478. ISSN: 0141-0296. https://doi.org/https://doi.org/10.1016/j.engstruct.2021.113478.

Kyburz, M. L., Sovilla, B., Gaume, J., and Ancey, C. (Feb. 2022b). The concept of mobilized domain: how it can explain and predict the forces exerted by a cohesive granular avalanche on an obstacle. In: Granular Matter 24 (2), p. 45. https://doi.org/https://doi.org/10.1007/s10035-021-01196-1.

Kyburz, M. L., Margreth, S., Berner, F., Sovilla, B., and Gaume, J. (Sept. 2024). "New Inferences on the Importance of slope-normal Snow Avalanche Velocity Components from depth-resolved Avalanche Simulations". In: International Snow Science Workshop, Tromsø, Norway. Tromsø, Norway, pp. 387–392.

Kyburz, M. L., Sovilla, B., Bühler, Y., and Gaume, J. (2025). Potential and challenges of depth-resolved three-dimensional MPM simulations: a case study of the 2019 'Salezer' snow avalanche in Davos. In: Annals of Glaciology 65, e19. https://doi.org/https://doi.org/10.1017/aog.2024.14.

Li, X., Sovilla, B., Jiang, C., and Gaume, J. (2020). The mechanical origin of snow avalanche dynamics and flow regime transitions. In: The Cryosphere 14.10, pp. 3381–3398. https://doi.org/https://doi.org/10.5194/tc-14-3381-2020.

Margreth, S. (2007). Snow pressure on cableway masts: Analysis of damages and design approach. In: Cold Regions Science and Technology 47.1. A Selection of papers presented at the International Snow Science Workshop, Jackson Hole, Wyoming, September 19-24, 2004, pp. 4–15. ISSN: 0165-232X. https://doi.org/https://doi.org/10.1016/j.coldregions.2006.08.020.

SIA261/1 (2020). Einwirkungen auf Tragwerke – Ergänzende Festlegungen (SIA 261/1). Schweizer Norm SIA 261/1:2020. Zürich: Schweizerischer Ingenieur- und Architektenverein (SIA).

Sovilla, B., Kern, M., and Schaer, M. (Jan. 2010). Slow drag in wet-snow avalanche flow. In: Journal of Glaciology 56.198, pp. 587–592. https://doi.org/https://doi.org/10.3189/002214310793146287.

Sovilla, B., Faug, T., Köhler, A., Baroudi, D., Fischer, J.-T., and Thibert, E. (Jan. 2016). Gravitational wet avalanche pressure on pylon-like structures. In: Cold Regions Science and Technology 126.Supplement C, pp. 66–75. ISSN: 0165-232X. https://doi.org/https://doi.org/10.1016/j.coldregions.2016.03.002.

Thibert, E. and Baroudi, D. (2010). Impact energy of an avalanche on a structure. In: Annals of Glaciology 51.54, pp. 45–54. https://doi.org/https://doi.org/10.3189/172756410791386634.

Thibert, E., Faug, T., Bellot, H., and Baroudi, D. (2013). "Avalanche impact pressure on a plate-like obstacle". In: International Snow Science Workshop, Grenoble–Chamonix, France, pp. 663–667.